Proceedings of the ASME 2020 39th International Conference on Ocean, Offshore and Arctic Engineering OMAE2020
June 28-July 3, 2020, Fort Lauderdale, FL, USA

OMAE2020-19183

LOW-HEIGHT LIFTING SYSTEM FOR OFFSHORE WIND TURBINE INSTALLATION: MODELLING AND HYDRODYNAMIC RESPONSE ANALYSIS USING THE COMMERCIAL SIMULATION TOOL SIMA

David Vågnes*, Thiago Gabriel Monteiro, Karl Henning Halse, Hans Petter Hildre
Department of Ocean Operations and Civil Engineering
Faculty of Engineering
Norwegian University of Science and Technology
6009 Ålesund

ABSTRACT

With the increasing demand for renewable energy sources in the past years, the interest in expanding the use of wind energy has grown. The next frontier in this expansion process is the use of floating wind turbines offshore. One of the main factors dictating the economic feasibility of such wind turbines is the complexity of their installation process. The dimensions of modern offshore wind turbines, the distance from the installation sites to the coast and demanding environmental factors all contribute to the difficult of developing an efficient installation concept for this kind of structures. In this work, we present a new concept for a catamaran vessel capable of handling the deployment of offshore wind turbines on floating spar platforms using a low-height lifting system that connects to the lower end of the wind turbine. The low-height lifting system is controlled by an active heave compensation system and constant tension tugger wires attached to the turbine mid-section are used to ensure the balance of the tower during the installation process. We conducted a series of hydrodynamic analysis using the software suit SIMA to study the dynamic response of the proposed system under different weather conditions and different operational layouts. This preliminary concept was proven feasible from a hydrodynamic point of view and can now be pushed forward for further studies regarding other aspects of the operation, such as impact and structural loads and mechanical design of components.

*Contact author: david.vagnes@ntnu.no

INTRODUCTION

Human influence on the climate system is very likely linked with the huge emission of greenhouse gases like carbon dioxide, methane and nitrous oxide [1]. This will have a widespread negative impact on natural and human systems, which motivates our behavior to better our emission of greenhouse gasses. As a consequence, a larger focus on renewable energy sources has emerged, which can be seen in the increase of installed capacity of offshore wind power in Europe [2]. In contrast to land-based wind turbines, offshore wind turbines (OWT) are regarded as an attractive solution due to higher wind speeds, more consistent wind patterns and less visual pollution in inhabited areas.

Within offshore wind, the vast majority of wind turbines are installed with bottom fixed monopile foundations. The economic viability of bottom fixed OWTs are great compared to land-based wind turbines, but they are limited to water depths of 50 m. For deeper waters, a floating foundation is needed. However, floating wind turbines (FWTs) are a relatively new concept, limited by their cost. For a typical offshore wind power plant, installation is a substantial part of the overall project cost. This is due to two main factors: the complexity of the installation process and the number of turbines to be installed. With a more effective installation method, the overall installation cost of an offshore wind park can be significantly reduced, making FWTs a more feasible solution.

In October 2017 the world's first floating wind turbine park, *Hywind Scotland*, was introduced by Equinor [3]. During the

first three months in full operation, Hywind performed much better than expected, with an average capacity factor of 65%. In comparison, bottom fixed wind turbines in similar areas reached a capacity factor of 45-60%. The wind turbine park consists of five 6MW wind turbines, adding up to a total production of 30MW. The wind turbines for Hywind were assembled onshore, lifted to a floating spar foundation by a heavy crane vessel in the sheltered Norwegian fjords, and then towed to their location at the coast of Scotland. Even though the installation cost of Hywind Scotland was greatly reduced compared to its predecessor *Hywind Demo*, a single 2.3 MW unit, the installation costs were substantial, motivating the development of more cost efficient installation methods.

For OWT installation, the tower, nacelle and blades can either be pre-assembled and handled in a single lift, or be installed part by part in several lifts. For other innovative installation concepts, pre-assembled wind turbines tend to be the preferred method, due to the complexity of performing the assembling operation offshore. A novel OWT installation concept was proposed by SFI MOVE [4], which utilizes a low-height lifting mechanism in order to avoid tall weather-sensitive heavy lifts. A catamaran vessel is arranged with two truss work lifting towers that move along the ship deck and use a grippers system to lift and deploy the OWT from the ship stern.

This work proposes an improvement over the previous gripper system, which presented a very complex mechanical structure subject to big dynamic loads. We will proceed with the idea of a low-height lifting mechanism, but we will use winches and wires, rather than grippers, to reduce structural requirements of the lifting system and improve the handling of the lifted OWT. Additionally, a balancing system has been added to the lifting crane, in order to stabilize the OWT during the lift. In this paper, we describe the proposed installation concept, detailing the installation vessel, spar foundation and OWT. Hydrodynamic analyses are performed to assess the vessel and spar responses. Finally, the proposed installation concept is evaluated considering a possible installation area in the North Sea.

THE LOW-HEIGHT LIFTING SYSTEM CONCEPT

The main idea behind the proposed concept is to avoid tall and weather-sensitive heavy lifts, since they increase the structural requirement of the lifting structure and installation vessel. Additionally, the lifting operation is harder to perform and there is a big increase in the size of the lifting structure. In order to ensure the high stability of the vessel transporting the OWT, a wide catamaran was selected as the installation vessel. The Catamaran is designed to carry four fully assembled OWT in upright position. In this work, we have not answered questions regarding structural design of the catamaran hull or mechanical couplings used to lock the wind turbine in position during transportation. In this phase, we are more interested in the hydrodynamic behavior

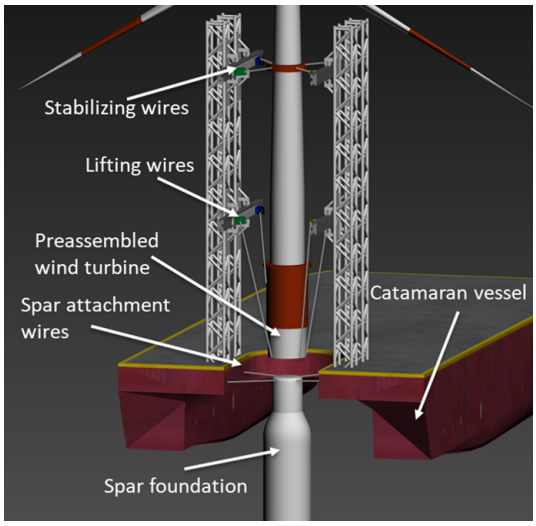

FIGURE 1: CATAMARAN OWT INSTALLATION CONCEPT.

of the proposed concept.

By carrying pre-assembled OWT, one decreases the number of required weather-sensitive lifting operations offshore. This implies a reduction in installation time, and thereby a reduction in cost. The lifting tower used for the operation is fitted with four wire winches capable of active heave compensation, which has the purpose of lifting and carrying the weight of the assembly. Low attachment points at the OWT bottom are utilized to allow for low lifting points on the Catamaran. In order to stabilize the OWT during the installation, a collar is wrapped around the upper part of the OWT and connected to the lifting towers by four wire winches, which then lock the OWT in the horizontal plane. The collar is equipped with skids in order to allow for vertical motions of the OWT.

During the wind turbine deployment from the vessel, it is desirable to control the Spar motion induced by the increase in draft caused by the wind turbine weight. For doing so, the Catamaran is arranged with four winches in the aft, which connects the vessel to the Spar foundation. This arrangement helps controlling the mating process by coupling the motions of the Catamaran and the Spar foundation.

All components of the installation concept are illustrated in Fig. 1, and selected parameters of the studied bodies are summarized in Tab. 1-3.

OWT installation procedure

The installation process relies on an already anchored Spar foundations at site. The anchoring is performed in advance by a specialized vessel. When the Catamaran arrives at site, the

TABLE 1: SELECTED PROPERTIES OF THE STUDIED OFFSHORE WIND TURBINE.

Parameter	Symbol	Value
Rated power (MW)	RP	10
Tower height (m)	H_{tower}	115.63
Rotor mass (tonnes)	M_{rotor}	227.96
Nacelle mass (tonnes)	$M_{nacelle}$	446.04
Tower mass (tonnes)	M_{tower}	628.44
Body origin in global coord. system	(x_w, y_w, z_w)	(0,0,0)

TABLE 2: SELECTED PROPERTIES OF THE STUDIED SPAR.

Parameter	Symbol	Value
Diameter at top (m)	L_{bd1}	9.5
Diameter at waterline (m)	M_{bd1}	14
Draft (m)	T_{s1}	70
Body origin in global coord. system	(x_s, y_s, z_s)	(0,0,0)
Vert. posit. of center of buoyancy (m)	Z_{sCOB1}	-35
Vert. posit. of COG (m)	Z_{sCOG1}	-51.8
Displacement mass (tonnes)	Δ_{s1}	11045

installation procedure is divided into nine main phases.

Phase 1 - The Catamaran is attached to the Spar by wires. The winches arranged in the aft of the Catamaran tension the wires and lift the Spar up, creating a strong coupling between the installation vessel and the floating foundation.
Phase 2 - Weather forecast and motion measurements are checked before the operation can proceed. Once the motions are considered safe, the operation can proceed.
Phase 3 - The lifting tower positions itself to the closest OWT. The lifting wires are attached to the bottom of the tower and the stabilizing wires to the mid-top section.
Phase 4 - The OWT is lifted and the path between the turbine and Spar is cleared.
Phase 5 - The OWT is then transported by the lifting tower along a rail system and positioned above the Spar.

TABLE 3: SELECTED PROPERTIES OF THE STUDIED CATAMARAN.

Parameter	Symbol	Value
Length overall (m)	L_{OA}	134
Breath moulded (m)	B	60.8
Spacing between mono-hulls at waterline (m)	L_{hull}	38
Draft (m)	T_c	8.0
Displacement mass (tonnes)	Δ_c	18525
Vert. posit. of COG abv. baseline (m)	KG_c	28.6
Body origin in global coord. system	(x_c, y_c, z_c)	(64,0,0)

Phase 6 - Once the OWT is placed above the Spar, the relative distance between the OWT bottom and Spar top is monitored with a Motion Reference Unit (MRU) or OCTOPUS system. This is done to decide whether the motion between the two bodies are within allowable limits for a safe and successful mating.
Phase 7 - When the relative motion is within an acceptable limit for a certain time interval, the mating between the OWT and Spar takes place. In order to increase the allowable limit of relative motion, an aligning system or docking pins are suggested, but not investigated in this paper.
Phase 8 - The bolting or welding process begins. The mating process is deemed successful once the OWT and Spar are successfully connected.
Phase 9 - The installation is finalized by the Catamaran lowering the Spar and assembled OWT with the winches in the aft. Each wind turbine has a weight of approximately 1100 tonnes, which would increase the draft of the platform by approximately 10 m. When the complete FWT is lowered to its new equilibrium position, the Catamaran detaches from the Spar, and moves to the next foundation, where the procedure is repeated.

SYSTEM MODELLING

The numerical modelling of the proposed installation concept faces three main challenges:

1. Structural dynamics: Since the installation process consists of three coupled rigid bodies, the system will exhibit several coupled eigenmodes. An understanding of how these modes affect the system dynamics is important and the eigenmode

TABLE 4: SELECTED PROPERTIES OF THE MOORING SYSTEM UNDER NO ENVIRONMENTAL LOADS.

Parameter	Symbol	Value
Diameter of upper chain (mm)	D_{upper}	132
Diameter of lower chain (mm)	D_{lower}	147
Submerged weight of upper chain (kN/m)	W_{upper}	3.69
Submerged weight of lower chain (kN/m)	W_{lower}	4.24
Product of elastic modulus and cross sectional area of upper chain (kN)	EA_{upper}	1.37E6
Product of elastic modulus and cross sectional area of lower chain (kN)	EA_{lower}	1.68E6
Pretension in the top segment (kN)	T_0	674

TABLE 5: CONNECTION WIRES PROPERTIES.

Parameter	Value
Connection flexibility (m/kN)	1E-4
Material damping (kNs)	7696.90
Wire cross section stiffness, EA (kN)	7.70E5

analysis will be discussed later on this paper.

2. Hydrodynamics: two wet bodies with distinct hydrodynamic properties are needed for the modelling of the concept. For the Catamaran, sloshing between the two mono hulls should be captured. In shallow waters, second order viscous hydrodynamic effects should be investigated. Also, interactions between the Catamaran and the Spar must be considered during the hydrodynamic loads calculation.
3. Control: Controlling the motion of several bodies by active heave compensation is challenging when none of the bodies is globally fixed.

Trying to address these issues, in this section we briefly describe how the proposed concept was modelled, including details about the Catamaran, Spar and OWT modeling as well as discussions about the active heave compensator (AHC) and environmental conditions implementation.

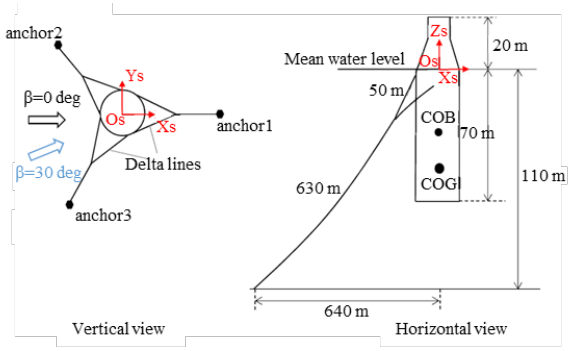

FIGURE 2: ILLUSTRATIVE LAYOUT OF THE MOORING SYSTEM FOR THE FLOATING SPAR FOUNDATION.

Modelling tools and methods

In this work, the hydrodynamic workbench SIMA is used for analyzing the proposed maritime operation concept. The multi-body system is modelled with features in the time-domain simulation software SIMO. Calculation of hydrodynamic coefficients was done with a combination of softwares in Sesam. A finite element panel model of the Spar and Catamaran was modelled in GeniE, and frequency domain analysis of the two stationary bodies was performed on the panel using Wadam, executed from the work environment of HydroD. A multi-body model is used in order to capture the hydrodynamic coupling between the bodies [5]. From the Wadam analysis, hydrodynamic coefficients like added mass, damping and stiffness matrix and hydrodynamic interaction coefficients like coupled added mass and damping between the bodies were determined for the time-domain analysis in SIMO. In addition to coefficients from potential theory, the Spar was fitted with empirical damping in heave and roll/pitch of 6.35E2 kNs/m and 5.35E5 kNm/(rad/s), respectively.

In SIMO, the Catamaran position keeping is achieved with a DP system consisting of four propellers, two acting as side and bow thrusters, and two acting as main propulsion. The DP system uses a Kalman-filter based controller and is set up so that the aft mating point of the Catamaran follows the body origin of the Spar. The Spar is moored with a mooring system composed by three catenary mooring lines, without delta lines. In order to represent the large yaw restoring from the absent delta lines, equivalent hydrostatic stiffness in yaw of 2.9E5 kNm/rad is applied on the Spar. Detailed properties of the mooring lines are listed in Tab. 4 and the mooring arrangement is illustrated in Fig. 2.

Simple wire coupling is utilized to model the wire connections between the bodies in the SIMO analysis. The required parameters to model the wires are listed in Tab. 5. The wires are regarded as steel wires with Young's modulus of 200 kN/mm^2 with 70 mm diameter. The material damping is taken as 1% of

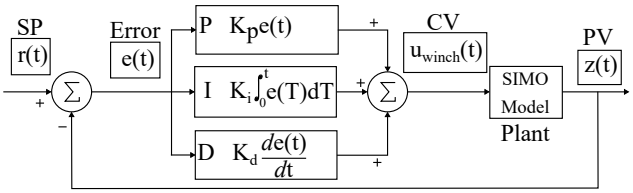

FIGURE 3: PID CONTROLLER USED TO CONTROL THE VERTICAL DISTANCE BETWEEN SPAR TOP AND OWT BOTTOM.

the wire cross section stiffness, according to SIMO documentation [6]. In order to prevent slack of wires, the wires are in a state of pre-tension in the initial position.

Active heave compensator modelling

The mating phase of the FWT installation has strong requirements regarding the relative movement between the OWT and the Spar. Following these requirements are essential to reduce the risk of high impact loads that could affect the structural integrity of either bodies or their connection interfaces. The accepted relative movement between the two bodies could be as low as some dozens of centimeters. Although this requirement could be naturally fulfilled in some sea states, it is important to have some kind of control mechanism to increase safety and operational window.

In this work we opted for implementing an AHC based on a PID controller to control the relative distance between the OWT bottom and the Spar top. Due to limitation in the kind of actuator we could implement in SIMO, in this stage of our study, we are only trying to control the vertical distance between the bodies. In this case we are using winches as actuators. The PID controller was implement using SIMO's Generic External Control System Interface. The controller was implemented in Java, and the control algorithm is run at every time step of the simulation.

The implemented controller is presented in Fig. 3. The process variable (PV) is defined as the actual vertical distance between OWT and Spar. PV is calculated using the pose (position plus orientation) of the two bodies. The set point (SP) is the desired vertical distance between OWT and Spar. The control variable (CV) is defined as the input velocities for the winches that control the lifting wires. Finally, the process Plant is the simulation performed in the SIMO environment. Due to the nature of the problem, the controller gains were tuned individually for the different wave frequencies.

Environmental conditions modelling

The proposed OWT installation concept is thought to operate in light wave conditions, in the North Sea. During the operation the Catamaran will be positioned aligned to the wave direction to reduce vessel response. We consider to have an operational window in the summer months (Jun-Aug), hence hindcast data for the central North Sea outside of the Scotland coast is extracted [7]. For the measuring grid point in this area, the percentage of exceedance distribution for significant wave height (H_s) during the summer months is summarized in Tab. 6. The wave height distribution shows that the wave height is not likely to exceed more than 2.5 m, which becomes the upper limit of the investigating environmental conditions (EC). Each significant wave height is related to an occurrence of spectral peak period (T_p) in this area, which is the basis for the selected environmental conditions for the wave spectrum simulations.

TABLE 6: ENVIRONMENTAL CONDITIONS (EC) IN THE CENTRAL NORTHERN SEA (56.748° N, 1.583° W), INCLUDING SIGNIFICANT WAVE HEIGHT, TYPICAL SPECTRAL PEEK PERIODS, AND PROBABILITY OF EXCEEDING SIGNIFICANT WAVE HEIGHT DURING SUMMER MONTHS.

EC	$H_s(m)$	$T_p(s)$	Jun (%)	Jul (%)	Aug (%)
1	0.5	3, 4, 5, 6, 7	83.58	80.80	56.70
2	1.0	4, 5, 6, 7, 8	39.17	30.86	39.75
3	1.5	5, 6, 7, 8, 9	10.31	7.86	14.64
4	2.0	5, 6, 7, 8, 9	1.76	1.49	4.51
5	2.5	6, 7, 8, 9, 10	0.48	0.03	1.25

SIMULATION RESULTS AND DISCUSSIONS

We want to investigate how the installation concept performs in the stage where the OWT is positioned above the Spar (Phase 7). The simulation consists of a total of three bodies. The Catamaran and Spar with associated hydrodynamic properties were modeled in previous work of the project [4]. The OWT is modeled as a simplified structure, where the tower, nacelle and blades are regarded as one single body with calculated mass properties given in Tab. 7. The Catamaran is considered ballasted, and a vertical force and pitch moment are applied in order to ensure an even keel during the mating process.

The environmental conditions are simulated in SIMA with the calculation engine SIMO. The water depth of the simulated location is set to 110 m and swell waves, wind and current are not included in the analysis. The simulation time for the time-domain analysis is set to 3600 s and the time step is set to 0.1 s, which is regarded as sufficient to correctly capture the simulation responses with acceptable computational complexity.

TABLE 7: MASS PROPERTIES OF THE STUDIED OFFSHORE WIND TURBINE.

Parameter	Value
Mass (tonnes)	1302.40
$COG(x,y,z)$ (m)	(-0.31, 0.00, 84.39)
I_{xx} (tonnes m^2)	1.25E7
I_{yx} (tonnes m^2)	0
I_{yy} (tonnes m^2)	1.25E7
I_{zx} (tonnes m^2)	47210
I_{zy} (tonnes m^2)	0
I_{zz} (tonnes m^2)	14640

In this section we present several analysis regarding the Phase 7 of the operation. We first performed an eigenvalue analysis to understand the coupling between the responses of the different bodies. Then, the response amplitude operators for Spar and Catamaran are calculated to present an overview of which kind of response we can expect from each body. Following, we present relative distances and wire forces analysis for regular waves, studying both the cases with and without AHC. Finally, we present a spectrum analysis which tries to reproduce the environmental conditions of the installation site of interest in the North Sea.

Eigenvalue analysis

An eigenvalue analysis of the three coupled bodies is conducted in frequency domain. This is done to characterize the basic dynamic behavior of the system and used as an indication of how the bodies will respond to dynamic loading. The eigenvectors and natural periods were found by solving the eigenvalue problem in Eqn. (1):

$$[-\omega^2(M+A)+C]\cdot X = 0 \tag{1}$$

where M, A and K are the mass matrix, added mass matrix and restoring stiffness matrix of the total system, respectively. X is the eigenvector that determines the mode of vibration and ω is the corresponding eigenvalue.

The modes related to the OWT are in the lower range of natural periods for the system. These periods are of such a low magnitude that they are not likely to be excited by the environment. The eigenvectors for the different modes show a coupling in translation and rotation for most of the modes, except the yaw mode of the OWT and Spar, which is approximately pure yaw, and heave mode for the Spar. The natural periods for the Catamaran and Spar in heave, pitch and roll are more likely to be excited by the environment, since they are in the range between 6.9-17.1 s. Tab. 8 presents selected eigenperiods and corresponding eigenvectors for the Catamaran, Spar, and OWT. The dominant modes for each frequency are highlighted.

TABLE 8: SELECTED EIGENMODES.

Body	Mode	5.25	5.40	7.24	11.67	14.07
Ship	η_1 (m)	-0.24	0.00	-0.40	0.10	-0.34
Ship	η_2 (m)	0.00	0.00	-0.01	-0.26	-0.22
Ship	η_3 (m)	0.31	0.00	**-1.00**	0.01	0.00
Ship	η_4 (deg)	0.02	0.00	0.00	-0.90	-0.57
Ship	η_5 (deg)	0.48	0.00	0.78	-0.20	0.59
Ship	η_6 (deg)	-0.03	0.01	-0.05	0.09	-0.05
Spar	η_1 (m)	-0.06	0.00	-0.10	0.03	-0.11
Spar	η_2 (m)	0.01	0.00	0.03	-0.02	0.05
Spar	η_3 (m)	-0.62	0.00	-0.49	-0.35	**1.00**
Spar	η_4 (deg)	-0.03	0.00	-0.04	0.02	-0.01
Spar	η_5 (deg)	-0.08	0.00	-0.13	0.03	-0.10
Spar	η_6 (deg)	0.46	**-1.00**	-0.10	0.10	-0.05
OWT	η_1 (m)	0.02	0.00	0.12	-0.06	0.16
OWT	η_2 (m)	-0.01	-0.01	0.04	-0.11	-0.02
OWT	η_3 (m)	**1.00**	0.00	0.05	-0.24	0.80
OWT	η_4 (deg)	-0.02	0.00	-0.01	**-1.00**	-0.65
OWT	η_5 (deg)	0.55	0.00	0.76	-0.15	0.45
OWT	η_6 (deg)	-0.02	0.02	-0.04	-0.02	-0.12

Response amplitude operator

In order to achieve a deeper understanding of the motion of the coupled system, response amplitude operators (RAO) for the Catamaran and Spar are created, both in a coupled and uncoupled system. In time-domain, this can be done by exposing the floating body to regular waves of 1 m amplitude, varying the period, and measuring the response amplitude of the desired motion for the current wave period. RAO for the uncoupled Catamaran and

Spar in heave and pitch with head sea and 30° sea are shown in Fig. 4.

The RAO of the Catamaran in heave shows small peaks and some cancellation effects that one would expect for a ship. This can be explained by investigating the expression for heave response in Eq. 2 which suggest cancellation when $sin(kL/2) = 0$, where $k = 2\pi/\lambda$ [8].

$$|\eta_3|_{\text{head sea}} = |\eta_3|_{\text{beam sea}} \cdot \frac{2}{kL}\left|\sin\left(\frac{kL}{2}\right)\right| \tag{2}$$

Using the expression for wave number k, we see that the sinusoidal function is zero for wavelengths $\lambda = L$, $\lambda = L/2$ and $\lambda = L/3$. Utilizing the relationship between wavelength and wave period, we see that cancellation occur for $T = 9.26$ s, $T = 6.55$ s and $T = 5.35$ s, which is equivalent to the calculated RAO in Fig. 4a.

In the pitch RAO of the Catamaran, we observe a peak at the pitch natural period $T = 10.5$ s, which is in agreement with the expression for the natural period of uncoupled motions in Eq. 3:

$$T_{n5}^{c} \sim 2\pi\sqrt{\frac{I_5 + A_{55}}{C_{55}}} = 9.2 \text{ s} \tag{3}$$

From the RAOs of the uncoupled Spar, it is important to note that the magnitude of response is not significant in the range of the investigated wave periods. This indicates that the pre-installed floating foundation will have relaxed response prior to coupling with the installation vessel. The response in heave and pitch peaks at the natural period of $T = 17$ s and $T = 30$ s, respectively. In addition to the peak at the natural period, the pitch RAO has a smaller peak which occur at $T = 16$ s stemming from the forcing wave frequency [9].

We are able to approximate the natural period of the Spar in heave with the theoretical expression in Eq. 4:

$$T_{n3}^{s} \sim 2\pi\sqrt{\frac{T_s}{g}\frac{d_{max}}{d_{min}}} = 16.8 \text{ s} \tag{4}$$

where T_s is the spar draft, g is the gravitational constant, d_{max} denotes the maximum diameter of the cylinder and d_{max} is the minimum diameter of the cylinder, which agrees with the analytical solution.

RAOs for the Spar and Catamaran are created for the coupled system as well and presented in Fig. 5. The RAOs for the Catamaran in the coupled system are somewhat changed in heave and pitch, but the general shape stays the same. We observe that

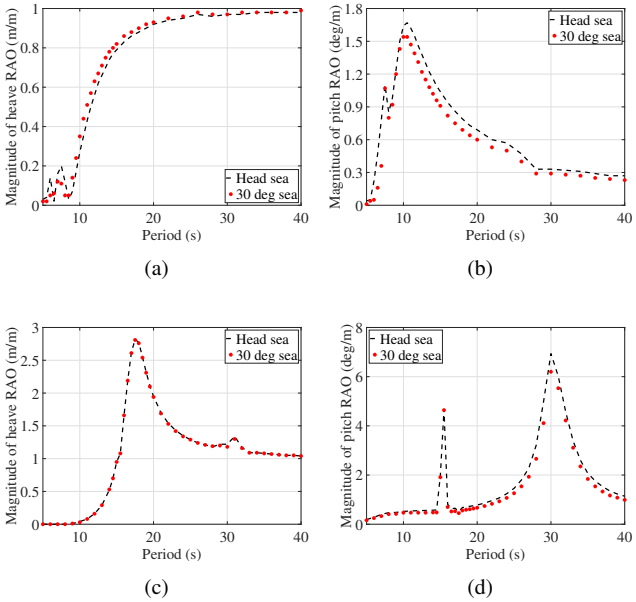

FIGURE 4: SELECTED RAOs OF THE FREELY FLOATING BODIES. (a) HEAVE MOTION OF THE CATAMARAN (b) PITCH MOTION OF THE CATAMARAN (c) HEAVE MOTION OF THE SPAR (d) PITCH MOTION OF THE SPAR

the natural period in pitch has moved to $T = 12$ s as a consequence of the increased mass inertia (I_5) and added mass (A_{55}) introduced by the coupled Spar.

In the coupled analysis, we observe that the RAOs of the Spar has changed significantly. Because of the strong wire coupling between the Catamaran and Spar, the pitch response of the Catamaran dominates the heave response of the Spar, making the two RAOs virtually identical. One would expect that the heave natural period at $T = 17$ s would have an impact on the pitch response of the Catamaran, but it remained unaffected. In addition, now two modes are present for the Spar in pitch because of the mechanical coupling between the bodies.

Relative distance

For a successful mating between the OWT and Spar, the relative motions between the two bodies need to be minimized. Large horizontal motions may cause misalignment and high stresses in the bolting, whereas large vertical motions may cause impact forces during the mating. The relative distance (η) between the center of the Spar top and OWT bottom is defined as the three-dimensional distance between the two points by Eq. 5:

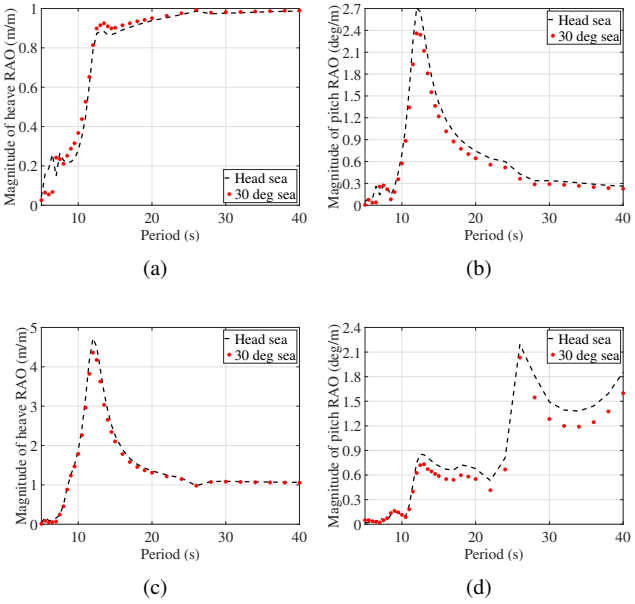

FIGURE 5: SELECTED RAOs OF THE COUPLED FLOATING BODIES. (a) HEAVE MOTION OF THE CATAMARAN (b) PITCH MOTION OF THE CATAMARAN (c) HEAVE MOTION OF THE SPAR (d) PITCH MOTION OF THE SPAR

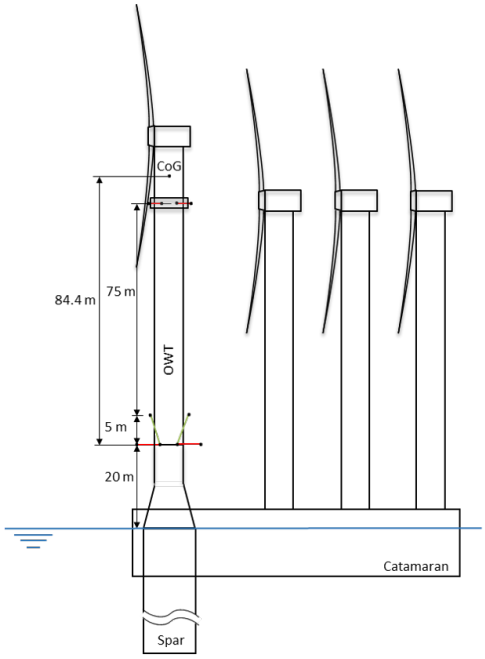

FIGURE 6: INITIAL PHASE OF THE MATING PROCESS.

$$\eta = \sqrt{(x_1 - x_2)^2 + (y_1 - y_2)^2 + (z_1 - z_2)^2} \tag{5}$$

where the indices 1 and 2 refer to the OWT bottom and Spar top respectively, and x, y and z are the coordinates.

Fig. 6 shows a conceptual drawing of the initial phase of the mating process (Phase 6), where the OWT is positioned just above the Spar. In this position, relative motions the two bodies are monitored and evaluated.

According to the principle of rigid body motions for small rotations, the motions in the mating point of the two bodies can be calculated by Eq. 6:

$$\begin{aligned}\hat{s} = {} & (s_1 + z_r s_5 - y_r s_6)\hat{i} + (s_2 - z_r s_4 + x_r s_6)\hat{j} \\ & + (s_3 + y_r s_4 - x_r s_5)\hat{k}\end{aligned} \tag{6}$$

where s_1 to s_6 are the rigid body motions of the Catamaran or Spar, and $(x_r,\ y_r,\ z_r,)$ is the position of the mating point for each individual body relative to its body origin. Simulations with varying wave periods are performed, and the relative distance between the center of the Spar top and OWT bottom is determined. Both the three-dimensional distance and the decoupled distances in x-, y-, and z-direction are calculated, and the resulting responses are presented as RAOs in Fig. 7.

When examining the response amplitude operators of relative distance between the Spar top and the OWT bottom, the motion analysis of the coupled bodies comes in very handy. The peak at $T = 12$ s in the heave RAO for the Spar is apparent both in the RAOs of x- and z-distance, which suggests that the peak is induced by pitch motion. Looking at the Catamaran pitch motion, we observe the very same peak in pitch for this period. In general, we observe that the relative distance between the two bodies are highly dependent on the Catamaran pitch, considering the shape of the respective RAOs.

Analyzing Fig. 7, it is noticeable that the total distance is dominated by the z-distance and the component from the x and y directions have little effects over it. In this case, the AHC implemented has a big effect reducing the vertical and, consequently, the total distances. In this analysis, the relative distance reduction was, approximately, in the range between 40-60% for the different periods. Regarding the possibility of collision between the OWT and the truss-frame, the amplitude of the OWT surge and sway is small, both with and without AHC, compared to the available clearance of 85 cm in the current cable arrangement.

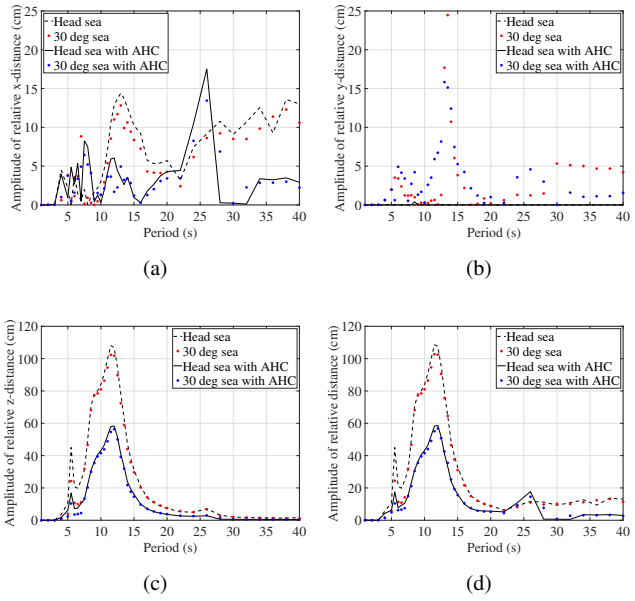

FIGURE 7: RELATIVE DISTANCE BETWEEN SPAR TOP AND WIND TURBINE BOTTOM RAOs. (a) X-DISTANCE (b) Y-DISTANCE (c) Z-DISTANCE (d) TOTAL RELATIVE DISTANCE η

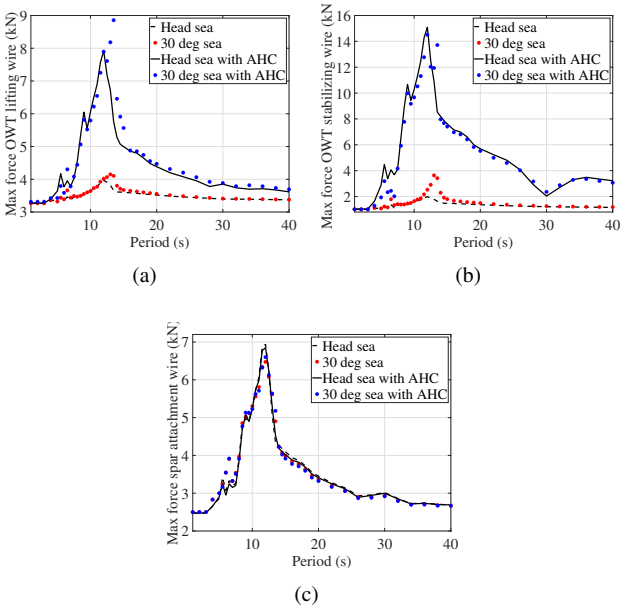

FIGURE 8: MAX FORCE IN THE THREE SETS OF WIRE COUPLINGS. (a) WIND TURBINE LIFTING WIRE (b) WIND TURBINE STABILIZING WIRE (c) SPAR ATTACHMENT WIRE

Wire forces

The concept utilizes three sets of four wires, one to lift the OWT, another to stabilize the assembly, and the last set to connect the Catamaran and Spar. During the analysis, forces in all individual wires are monitored and the maximum forces in each set are reported in Fig. 8. The model is exposed to regular waves with amplitude ζ_a=1 m and varying wave period. During the numerical simulations, no zero wire force events were observed, which indicates no occurrence of case of slack in the wires.

The plots show the results for concept with and without AHC. We observe that for the wire sets related to the OWT and, consequently, the AHC experience much bigger force when the AHC is activated. This is due to the fact that the AHC tries minimizing the distance in the mating point by shortening or lengthening the lifting wires. This results in an increase of the OWT acceleration, implying a larger dynamic amplification factor, leading to an increase of the wire forces.

Still for the set of lifting wires on the OWT, we observe an increase of maximum force as the motion of the Catamaran increases and dynamic load effects becomes more evident. Similarly, the force in the stabilizing wires increase with increase in motion. As the Catamaran pitches, the OWT is leaning forward or backwards depending on the pitch angle. This makes the stabilizing wires carry part of the weight of the OWT, which increases the restoring force in the wires.

As with the two other wire sets, the biggest forces in the Spar attachment wires occur when the motions between the bodies are the biggest. This set of wires experience the biggest magnitude of force, due to a combination of the large displacement of the Spar and the impact of wave induced forces on the bodies. Even though the forces in these wires are relatively big, conventional steel wires are still able to withstand this amount of force.

Environmental condition

For modeling the environmental conditions at site, irregular waves are generated using a JONSWAP wave spectrum. In addition to the parameters from Tab. 6, cosine spreading function with exponent $n = 2$ is used for the directional short-crested wave spectrum, according to recommended practice [10]. For this investigation, swell waves, wind and current are not included in the analysis. Five simulations with random wave seeds are performed for each environmental condition, and the results are based on the average response.

For the simulation of environmental conditions, the concept utilize AHC in order to reduce the motion in the mating point. The bar charts in Fig. 9 shows the maximum distance amplitude, standard deviation and mean distance from the mating point, as

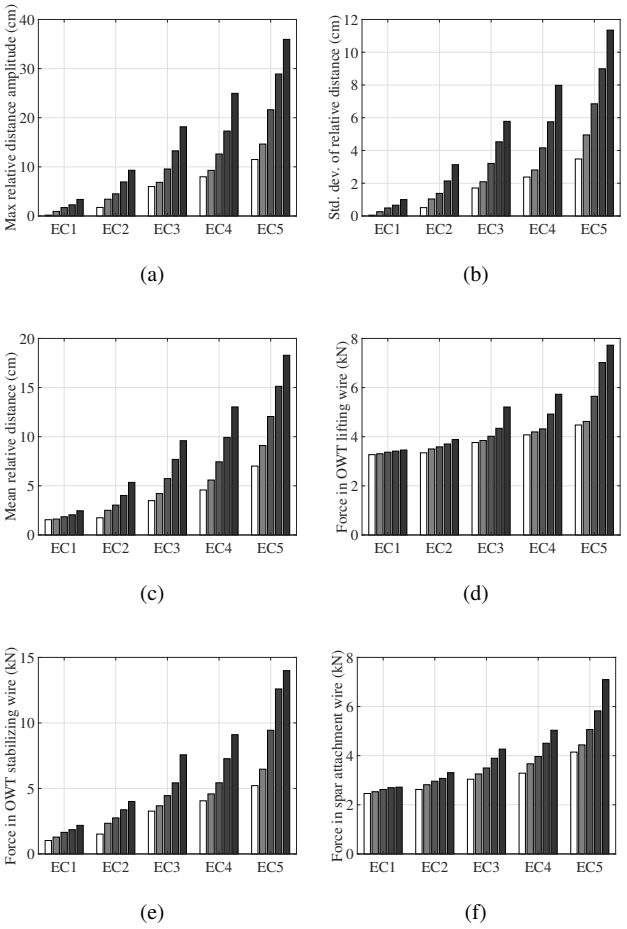

FIGURE 9: STATISTICAL VALUES AND WIRE FORCES DURING ENVIRONMENTAL CONDITIONS. (a) MAX RELATIVE DISTANCE AMPLITUDE (b) STANDARD DEVIATION RELATIVE DISTANCE (c) MEAN RELATIVE DISTANCE (d) MAX OWT LIFTING WIRE FORCE (e) MAX OWT STABILIZING WIRE FORCE (f) MAX SPAR ATTACHMENT WIRE FORCE

well as maximum force in the three wire sets. Selected environmental conditions are represented as groups, and labeled accordingly, and each individual bar in the groups represents the varying spectral peak period in ascending order. Using EC1 as an example, the bars in the group from left to right, represents $T_p = 3$ s, $T_p = 4$ s, $T_p = 5$ s, $T_p = 6$ s and $T_p = 7$ s.

For the two lightest environmental conditions (EC1 and EC2), we observe relatively small amplitude of motion in the mating point, as well as forces in the lifting-, stabilizing- and attachment wires. Reading from the coupled bodies RAO of the catamaran and floating spar, we expect very little motion for the current spectral peak periods of these environmental conditions, which also is the case for the measurements of the relative motion in the mating point. When the motion of the system is small, the dynamic load factor is expected to be small, and the force in a single OWT lifting wire can be approximated by the simplified expression in Eq. 7:

$$F_{OWT}^{LW} \sim \frac{M_{TOT}}{4} = 3.2 \text{ kN} \tag{7}$$

where M_{TOT} is the total mass of the OWT, which coincide with the maximum force in the lifting wire.

Assessing all the bar plots in Fig. 9 we observe that an increase in H_s also gives an increase of motion in the mating point, as well as forces in the wire sets. Looking at the relative distance for EC3 ($H_s = 1.5$ m) and EC4 ($H_s = 2.0$ m) in Fig. 9a-9c, we read that the bars representing the largest H_s has the biggest response. Similarly, the forces in the wire sets of Fig. 9d-9f shows the same behavior of increasing H_s.

For all environmental conditions we have increasing response in the mating point and forces in the wire sets, as the peak period approaches the resonance period of the coupled Catamaran in pitch and coupled Spar in heave.

CONCLUSION AND FUTURE WORK

This study assessed a catamaran offshore wind turbine installation vessel, utilizing a low height wire lifting system with active heave compensation. Numerical modelling and time domain simulation of the concept in SIMA gave the following main conclusions:

- The system has several natural periods. The ones related to the OWT are very low and are not likely to be excited at a common installation site. Natural periods for the Catamaran and Spar in heave, pitch and roll are more likely to be present during installation.
- RAOs were calculated for both uncoupled and coupled floating bodies. The pitch RAO of the Catamaran and heave RAO of the Spar appeared to be similar with the wire coupling. In pitch, two modes were present for the Spar RAO.
- With AHC, a reduction of the relative distance in the mating point was achieved. As a side-effect of the AHC, more force in the wire couplings related to the OWT was observed.
- The model was exposed to five environmental conditions with varying significant wave heights and spectral peak periods. Greater responses of relative motion in the mating point and wire forces are associated with increasing wave height and period.

The focus in this paper has been the positioning phase of the OWT, prior to mating with the Spar is studied. In a future study,

the lowered and final position of the OWT will be assessed. Although the AHC provided a considerable decrease in the total distance between the Spar top and OWT bottom, a more robust control algorithm is required to ensure the feasibility and safety of the operation. The properties used for the wire sets have been preliminary chosen, and further study will a more detailed modelling of the wires properties. Finally, more realistic environmental conditions need to be considered in a future work. Although only waves are modelled in this work, current and wind also have a significant impact on the OWT installation. For correctly capturing the effects of wind fields, a more realistic OWT model is required.

REFERENCES

[1] Pachauri, R. K., and Meyer, L., 2014. Synthesis report. contribution of working groups i, ii and iii to the fifth assessment report of the intergovernmental panel on climate change.

[2] Selot, F., Fraile, D., and Brindley, G., 2019. The european offshore wind industry - key trends and statistics 2018. Tech. rep., WindEurope.

[3] Equinor, 2018. Word's first floating wind farm has started production. https://www.statoil.com/en/news/worlds-first-floating-wind-farm-started-production.html. Accessed: 2019-12-12.

[4] Jiang, Z., Gao, Z., Halse, K. H., and Hilder, H. P., 2018. "Dynamic response analysis of a catamaran installation vessel during the positioning of a wind turbine assembly onto a spar foundation". In Marine Structures 61.

[5] DNV GL, 2019. Sesam user manual.

[6] SINTEF Ocean, 2018. SIMO 4.14.0 theory manual.

[7] Fugro Geos, 2001. Wind and wave frequency distributions for sites around the british isles.

[8] Faltinsen, O., 1993. *Sea loads on ships and offshore structures*, Vol. 1. Cambridge university press.

[9] Lyu, G., Zhang, H., and Li, J., 2019. "Effects of incident wind/wave directions on dynamic response of a spar-type floating offshore wind turbine system". *Acta Mechanica Sinica,* ***35***(5), Oct, pp. 954–963.

[10] Det Norske Veritas, 2010. DNV-RP-C205: Environmental conditions and environmental loads.